Intracellular pH in Single Motile Cells

JEANNE M. HEIPLE and D. LANSING TAYLOR
Cell and Developmental Biology, Harvard University, Cambridge, Massachusetts 02138

ABSTRACT Cytoplasmic pH in single living specimens of *Chaos carolinensis* is determined microfluorometrically by measuring the ratio of fluorescence intensity of microinjected fluorescein-thiocarbamyl (FTC)-ovalbumin at two different excitation wavelengths. The probe is evenly distributed throughout, and confined to, the cytoplasm, and the fluorescence intensity ratio depends only upon pH. It is independent of pathlength, concentration of probe, divalent cations, and ionic strength. Ratios are calibrated with a standard curve generated *in situ* by adjusting internal pH of FTC-ovalbumin-containing amebae with weak acid and weak base or by injection of strong buffers. With this technique, the average cytoplasmic pH of freely moving amebae is found to be 6.75 (SD ± 0.3). The pH of a given spot relative to the morphology of a moving ameba remains fairly constant (± 0.05 U), whereas the pH of two different spots in the same cell may differ by as much as 0.4 U, and average pH in different amebae ranges from 6.3 to 7.4, with a suggestion of clustering about pH 6.5 and 6.8. During wound healing, there is a local, transient drop in pH (as great as 0.35 U) at the wound site upon puncture, proportional in extent to the degree of damage. Comparison of tails and advancing pseudopod tips reveals no significant difference in cytoplasmic pH at this level of spatial (50 μm diameter spot) and temporal (1.3 s) resolution. Fluctuations in intracellular pH and/or intracellular free Ca^{++} may be involved in regulation of cytoplasmic structure and contractility.

Many lines of evidence support the current belief that Ca^{++} and/or pH serve as important secondary messengers in a variety of cell processes, such as ameboid movement (26), sperm and egg activation (12, 21, 30), muscle contraction (33), and secretion (reference 20 and footnote 1). These ionic parameters may exert their effect in part by directly altering the structure, activity, or interactions of the contractile proteins implicated in each event. For example, it has been demonstrated that gelation and contraction of single-cell models (27) and bulk extracts from amebae are regulated by changes in free Ca^{++} concentration (4, 10, 19, 34) and pH (4, 10). During extension of the acrosomal process in echinoderm sperm, a rise in pH apparently triggers actin polymerization, whereas an increase in intracellular free Ca^{++} appears to be necessary for membrane fusion events (30). Similarly, during egg activation, both a well-documented pH rise (12, 21) and a wave of increased free Ca^{++} concentration (8, 23) appear to play a role in early cortical events, including fusion of cortical granules and the elongation of actin-filled microvilli. Recently, working with isolated, unfertilized-egg cortices, Begg and Rebhun (1) showed that a rise in pH, similar to that thought to occur upon fertilization (12, 21), can induce the transformation of amorphous cortical actin to a filamentous form, and that this transformation is not sensitive to changes in free Ca^{++} concentration. Furthermore, studies with Triton-extracted muscle cells have shown that raising the pH from 7.0 to 7.7 at subthreshold Ca^{++} concentrations can induce contractions as effectively as raising the free Ca^{++} concentration to the threshold level (24).

Investigation of these cellular events and the signals responsible for them is complicated by our ignorance of the intracellular environment. The present work is aimed at determining cytoplasmic pH in single motile cells and investigating the possible relationships among pH, free Ca^{++}, and contractility. We have chosen the giant, free-living ameba, *Chaos carolinensis*, for this initial study because it is a large (average diameter 600 μm), easily manipulated cell that exhibits a variety of well-studied movements. Contractile proteins from *Chaos* have been partially characterized biochemically (3), and the distribution of fluorescently labeled actin has been followed after microinjection into living cells (28). Moreover, the concentration of free Ca^{++} has been mapped in these cells via luminescence of microinjected aequorin (25).

Special problems arise when one tries to measure pH and pH changes in different places in a single, rapidly moving cell. Use of a microelectrode is best suited to static cells or tissues. Distribution of a weak acid, such as 5,5-dimethyl-2,4-oxazolidinedione, is ideal for isolated, homogeneous vesicle populations or for obtaining an average intracellular pH that includes all the organelles and the cytoplasm (for review, see reference

[1] Horne, W. C., L. E. Tanoue, A. M. Laband, and E. R. Simons. 1980. Correlation of the thrombin-induced changes in the transmembrane potential, transmembrane pH gradient, and serotinin secretion of human platelets. Manuscript in preparation.

31). The latter limitations apply equally to the distribution of most pH-sensitive indicator dyes. Incorporation of pH-sensitive fluorescent probes has been successfully applied to cell suspensions (references 7, 17, and 29 and footnote 1) and to suspensions of subcellular particles (5, 6, 13), but not to the study of single cells or of localized changes within them.

Our approach has been to use an optical technique to quantitate fluorescence of fluorescein-thiocarbamyl (FTC)-ovalbumin after microinjection into single living amebae. The sensitivity of fluorescein fluorescence to physiologic pH is well documented (14), and the ratio of fluorescence intensities from a sample excited at two different wavelengths is independent of optical pathlength and of concentration of the probe (17, 29). Other advantages of this optical ratio technique include increased sensitivity and specificity for pH, minimal perturbation of the cell, and improved temporal and spatial resolution, because the soluble protein conjugate of the dye is confined to the cytoplasm, with no leakage and only slow, if any, uptake into subcellular compartments.

MATERIALS AND METHODS

Materials

Chaos carolinensis, obtained from Carolina Biological Supply, Burlington, N. C., are cultured in Marshall's medium (5×10^{-5} M $MgSO_4$, 5×10^{-4} M $CaCl_2$, 1.47×10^{-4} M K_2HPO_4, 1.1×10^{-4} M KH_2PO_4, pH 7.0) with mixed ciliates, as previously described (27). Ovalbumin is labeled with fluorescein isothiocyanate (FITC), isomer 1, obtained from Sigma Chemical Co., St. Louis, Mo., as described previously, (32) and the dye-to-protein ratio is estimated to be 1.8 (using a molar extinction coefficient of 68,000 at 495 nm, pH 8.0, for bound fluorescein). Spectral characteristics of the probe in solution are measured with a SPEX Fluorolog (Spex Industries, Metuchen, N. J.) and microfluorometrically (see below). The pH of all solutions is measured with a VanLab Ag/AgCl Combination Microprobe Electrode (VWR Scientific, San Francisco, Calif.) on a Corning Model 10 pH meter (Corning Glass Works, Science Products Div., Corning, N. Y.). Glass-distilled water and reagent grade chemicals are used throughout this work.

Microinjections and Microfluorometric Measurements

Amebae are pressure-microinjected, as described elsewhere (28), with approximately one-tenth cell volume of 3.0 mg/ml FTC-ovalbumin in a carrier solution of 2.5 mM PIPES, pH 6.95. The apparatus for measuring fluorescence intensity from the injected cells was designed in collaboration with Bob Zeh of Custom Instrumentation, N. Y., and is diagrammed schematically in Fig. 1. On a Zeiss Photomicroscope equipped with epiillumination, light from a 12 V/60 W quartz-halogen lamp passes through one of two interchangeable narrowband excitation filters and is reflected by the dichroic mirror to the sample. The excitation filters (496 or 452 nm interference filters, bandwidth at 50% T_{max} 11 and 14 nm, respectively, Feuer Optics, Upper Montclair, N. J.) are rapidly changed (0.5 s at each position, 0.3 s change-time) by a Superior Slo-Syn stepping motor (The Superior Electric Co., Bristol, Conn.) controlled by a KIM I Microprocessor. Fluorescent light collected by the objective from the sample then passes through the dichroic mirror, a variable aperture, and through a broad-band barrier filter (520–560 nm, Zeiss LP520 and KP560), and impinges on a photomultiplier tube (RCA Solid State, Sommerville, N.J.) where the signal is converted into a deflection on a chart recorder (Hewlett-Packard Co., Palo Alto, Calif., model 7132A). Note that the barrier filter has been placed above the eyepiece in front of the photomultiplier. This allows simultaneous fluorescence measurement and observation of the cell in transmitted bright-field light. A 645-nm interference filter (PTR Optics, Waltham, Mass.) is placed over the substage light source so that the barrier filter can prevent this light from reaching the photomultiplier. Measurements reported here are made with a Zeiss 25 × Pol Neofluar objective (NA 0.6) and an aperture, or spot size, of 50 or 75 μm in diameter (as specified in the text).

In each case, the ameba and observation chamber are first measured for background fluorescence. The ameba is then injected and allowed to recover for a few minutes. The fluorescence intensity at the two excitation wavelengths is measured while the cell is unperturbed and moving freely or after experimental manipulation. After correction for background fluorescence at each wavelength, the ratio of fluorescence intensities, Ex_{496}:Ex_{452}, is calculated for each measurement. Calibration of these ratios is described in Results. Image intensification and recording is carried out as described elsewhere (28).

RESULTS

Distribution of FTC-ovalbumin

Fig. 2 shows a fluorescence micrograph, obtained by image intensification, of a typical moving, FTC-ovalbumin–containing ameba, with a scale drawing of the measuring spot (50 μm diameter) superimposed upon it. Within seconds after injection, the FTC-ovalbumin appears to be uniformly distributed throughout the ameba's cytoplasm. Vacuoles, vesicles, and organelles appear dark against a fluorescent background of cytoplasm. Occasionally, two or three bright vesicles, presumably containing labeled protein, are observed to form near the site of injection. These brighter vesicles rarely increase in number over time and then only very slowly. In fact, the cytoplasm of amebae observed several days after microinjection is usually still fluorescent. This observation is similar to the slow rate of autophagy of rhodamine-conjugated ovalbumin observed after microinjection into HeLa cells (22). Thus, we are confident that, for the duration of our experiments, the FTC-ovalbumin is primarily confined to the cytoplasm, with insignificant uptake into vesicles or organelles. Moreover, the labeled ovalbumin diffuses quickly out of ruptured amebae (28), indicating its random, unbound distribution in the cell.

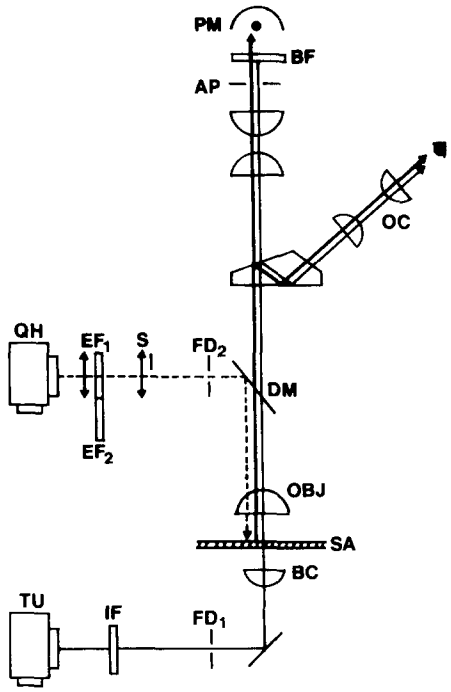

FIGURE 1 Schematic representation of the microfluorometer used to quantitate fluorescent signals. The dotted line represents the epiexcitation light from a quartz-halogen lamp *(QH)*, the heavy solid line represents the path of fluorescent light from the sample *(SA)*, and the lighter solid line represents light from a substage tungsten lamp (TU). A substage interference filter *(IF)* selects a wavelength of light, for bright-field observations, that will not pass through the barrier filter *(BF)* to the photomultiplier *(PM)*. Only fluorescent light from the sample passes through the barrier filter. Two interchangeable excitation filters (EF_1 and EF_2) select the wavelength of the excitation light. These are powered by a microprocessor-controlled stepping motor (not shown). A moveable shutter (S) allows the excitation light to be blocked when desired. Other symbols are as follows: FD_1 and FD_2, field diaphragms; *DM*, dichroic mirror; *OBJ*, objective; *BC*, bright-field condensor; *OC*, ocular; *AP*, variable aperture. The photomultiplier is connected to a chart recorder (not shown). See text for further details.

Standard Curves

Standard curves of the ratio of fluorescence intensity vs. pH for FTC-ovalbumin *in situ* (*a*) and in vitro (*b*) are shown in Fig. 3. We have chosen to generate these curves from pH 6.0 to pH 8.0, inasmuch as this is the range of cytoplasmic pH suggested by the literature (31). As the pH increases from 6.0 to 8.0, the ratio (Ex_{496}/Ex_{452}) also increases (on the *in situ* curve, from 7.00 to 10.7 and on the in vitro curve, from 3.90 to 9.60). Signals from cell-incorporated dyes or probes are usually calibrated by standard curves generated in solution, with little attention given to the possibility that the dye or probe used might behave quite differently in the cell environment. We find that the standard curve of FTC-ovalbumin in solution is a poor approximation of the one generated *in situ* by collapsing ΔpH across the membrane of an injected ameba with weak acid or base, as suggested by the work of Pollard et al. (18). Although similar in shape to the *in situ* curve, significantly different ratios are obtained for the range of pH values tested. In the range near neutrality, errors of up to 0.7 pH U can be incurred by calibrating ratios from injected cells with the standard curve generated in solution. Therefore, in all experiments reported here, fluorescence intensity ratios from injected cells were calibrated with the *in situ* standard curve.

Two methods are used for the generation of the *in situ* curve. In the first method, represented by solid symbols in Fig. 3 *a*, the internal pH of an injected ameba is equilibrated with an external pH determined by 10 mM PIPES, 10 mM HEPES, or 10 mM Tris-maleate buffers using 100 mM K acetate or 50 mM $(NH_4)_2SO_4$ as described previously (18). Though weak acids or bases are often used, at much lower concentrations, to determine average intracellular pH, at these higher concentrations they can be used to equilibrate internal and external pH (18). An important assumption in the pH equilibration technique is that the contribution of cellular constituents to the acid-base equilibria is negligible compared with the large excess of acid or base used to collapse the gradient. To corroborate these values, some amebae containing FTC-ovalbumin are injected with a minimum[2] of 1/10 cell volume of 100 mM Tris-maleate, 100 mM PIPES, or 100 mM HEPES buffers at a known pH, then measured (Fig. 3 *a*, open circles). These values concur with the acid-base equilibration method.[3] The buffering

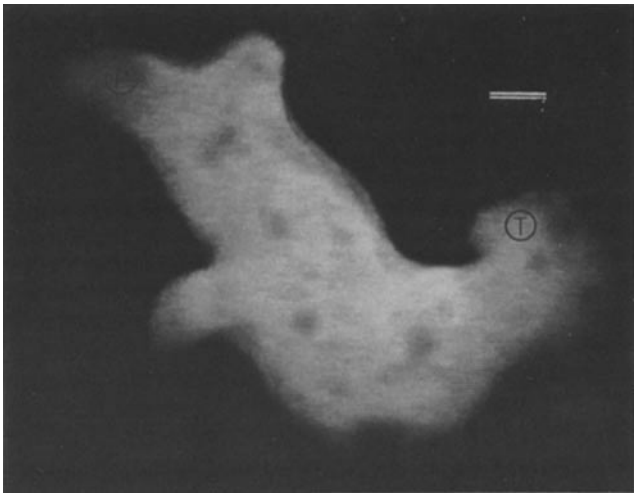

FIGURE 2 A specimen of *Chaos carolinensis* injected with FTC-ovalbumin, photograph of intensified video image. The fluorescent probe is evenly distributed throughout the cytoplasm and is excluded from the organelles, which appear dark. The ameba is moving toward the upper left-hand corner. Drawings of the measuring spot are superimposed upon the photograph in typical positions in an advancing pseudopod tip (*P*) and in the tail (*T*). Bar, 100 μm.

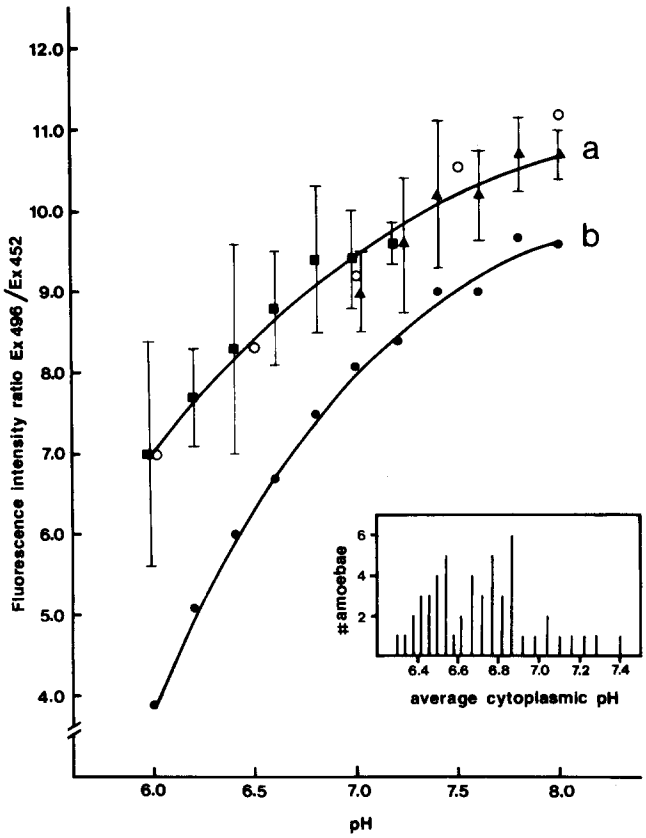

FIGURE 3 Standard curves of fluorescence intensity ratio (Ex_{496}: Ex_{452}, $Em_{520-560}$) vs. pH for FTC-ovalbumin *in situ* (*a*) and in solution (*b*), as measured with the microfluorometer diagrammed in Fig. 2. ■, FTC-ovalbumin-injected amebae equilibrated in 10 mM Tris-maleate (pH 6.0–7.2), 100 mM K-acetate or in 10 mM PIPES (pH 6.4–7.2), 100 mM K-acetate. ▲, FTC-ovalbumin-injected amebae equilibrated in 10 mM Tris-maleate (pH 7.0–8.0), 50 mM $(NH_4)_2SO_4$ or 10 mM HEPES (pH 7.0–7.8), 50 mM $(NH_4)_2SO_4$. Time-courses show that the pH stabilizes at the new value within 2 min with ammonia and within 7 min with acetate (data not shown); therefore, the latter value is used as a minimum incubation time. Each solid symbol in (*a*) represents an average of 6–13 amebae, with the single exception of three amebae at pH 6.2, for a total of 83 amebae. Vertical bars represent SD for these points. ○, FTC-ovalbumin-injected amebae injected with ≥1/10 cell volume of 100 mM Tris-maleate (pH 6.0–8.0), 100 mM HEPES (pH 8.0), or 100 mM PIPES (pH 7.0). Each point represents an average of two to four amebae; SD have been omitted for clarity, but in all cases they are smaller than those obtained by equilibration. ●, Solutions of 0.3 mg/ml FTC-ovalbumin in 10 mM Tris-maleate (pH 6.0–8.0) in silica-glass microcuvettes (Vitro-Dynamics, Rockaway, N. J.), averages of three samples each. *Inset*, a bar graph of the distribution of average cytoplasmic pH among 52 FTC-ovalbumin-injected amebae measured by this technique (using the *in situ* curve [*a*]). The values appear to form two groups, one clustered about pH 6.5, the other clustered about pH 6.8.

[2] More frequently, one-third cell volume or more is injected, as estimated from visual inspection of increased cell size, and decreased fluorescence intensity when buffers at pH 7.0 are injected.

[3] Preliminary attempts to generate this standard curve using the proton ionophores nigericin/K^+ or carbonyl cyanide *m*-chlorophenyl hydrazone (CCCP) were unsuccessful. In fact, CCCP quenches FTC-ovalbumin fluorescence.

capacity of ameboid cytoplasm is estimated to be ~11 meq H^+ ions/U pH change/liter, from titration of a homogenate of *Dictyostelium discoideum* amebae. Because the buffering capacity of 100 mM Tris-maleate (the most frequently used buffer) is 50 meq H^+ ions/U pH change/liter, it might not, when diluted by injection, be strong enough to overcome the buffering capacity of the cytoplasm. Therefore, buffer injections were repeated with 500 mM Tris-maleate at pH 6.0, 7.0, and 8.0 (data not shown). The average ratios obtained agree very well with those obtained by the injection of 100 mM buffer, indicating that the buffering capacity of the cell has been overcome in these experiments.

Of interest in these experiments is the reaction of amebae to the injection of strong buffers of various pHs or to equilibration in buffers of various pHs. In all cases, amebae respond initially by stopping and rounding up slightly. Then, if the buffer pH is between 6.0 and 6.8, the entire ameba forms a solid, gelled mass of evenly distributed organelles. This gelled state possesses great tensile strength, as can be observed by probing and stretching it with a microneedle and as implied by the ability of amebae to withstand the injection of buffer half or more of the original cell volume at these pHs. However, if the buffer pH is between 6.8 and 8.0, the cytoplasm appears to contract violently, increasing in intensity and speed with increasing pH, until it forms a dense knot in the center of the cell, leaving a border cleared of organelles under the membrane (an identical reaction is provoked by injecting Ca^{++} [25]). In this state, amebae are extremely fragile; they rupture easily and are more difficult to inject with large volumes of buffer.

The fluorescence intensity ratio of FTC-ovalbumin in solution is not significantly affected by ionic strength (0–200 mM KCl), [Mg^{++}] (0–1.0 mM) or [Ca^{++}] (10^{-8}–10^{-5} M), type of buffer (100 mM PIPES, HEPES, Tris-maleate, or Na-phosphate), 100 mM K^+ acetate, 50 mM $(NH_4)_2SO_4$, or photobleaching (data not shown).

Average Cytoplasmic pH and Variations

Average cytoplasmic pH is measured by sampling many regions (a minimum of nine) in a given cell, with a spot size of 50 or 75 μm in diameter, and averaging the values obtained. The distribution of average cytoplasmic pH among 52 amebae thus measured is shown in Fig. 3, *inset*. These amebae appear to cluster into two distinct groups, one with a slightly lower average pH (~6.5) than the other (~6.8). The cumulative average of all average cytoplasmic values is 6.75 (SD among amebae of ±0.30). Control experiments show that, in Marshall's culture medium, varying the extracellular pH from 6.0 to 8.0 has no measurable effect on intracellular pH, even after overnight incubation at these values.

The Wound-healing Response

Changes in cytoplasmic pH during the wound-healing response in *Chaos* are summarized in Fig. 4, which illustrates pH vs. time for a 50 μm diameter spot on the side of an advancing pseudopod of a typical ameba. The preinjected ameba is pricked from the side with a fresh, empty glass microneedle, which is immediately removed. Fluorescence intensity is recorded continuously before, during, and after the puncture. There is a slight, transient drop in pH at the wound site upon puncture (Fig. 4, arrow) that increases in extent with the degree of damage. In this cell, the pH drops from 7.25 to 6.90, and then recovers within 5 s to its original value. Though this ameba is found to have an average cytoplasmic pH of 6.85, the pH of this particular region of the cell is maintained before and after injury at 7.25 (SD ± 0.08). Similar results have been obtained from six other such experiments, though the magnitude and duration of the pH decrease varies slightly. In one experiment, no pH change was observed upon wounding the cell.

Comparison of Tails and Pseudopods

To investigate the possibility that the variations in cytoplasmic pH described above might be related to movement of the cell, we have undertaken a systematic comparison of average pH in tails and advancing pseudopods. Only freely moving, monopodial amebae are used for these experiments.

Chaos exhibits a well-known sensitivity to blue light (11). After ~3 s of exposure, advancing pseudopod tips stop and then either recover or reverse their streaming direction to become tails. Often, pseudopods will reverse streaming direction for a few seconds, then recover their original direction of motion (especially if the duration of exposure to blue light is brief). In contrast, tails are much less sensitive to blue light and will continue to move in the same direction. Because of this light-induced response, two different kinds of experiments are performed to examine the role of pH in the tail-pseudopod transformation, and are summarized in Fig. 5.

In the first kind of experiment, the fluorescence ratio (Ex_{496}/Ex_{452}) in a 50 μm diameter spot at the advancing edge of a pseudopod (see Fig. 2) is measured throughout the light-induced response: before the pseudopod stops, while it is stopped, upon streaming reversal, and again upon recovery (Fig. 5, arrows). Between measurements, the excitation light is blocked by a shutter (Fig. 1 *S*) to prevent excessive photo-damage to the cell. pH vs. time from a typical experiment is plotted in Fig. 5 *a*. No significant pH change is observed upon pseudopod arrest, reversal, or recovery in 16 experiments performed on seven monopodial amebae. If initial and final pH (after recovery) are compared for these pseudopods, an average drop of 0.02 U is observed during the course of the experiment, which does not exceed the average variation (±0.02 U) usually observed for a given spot over a similar period of time.

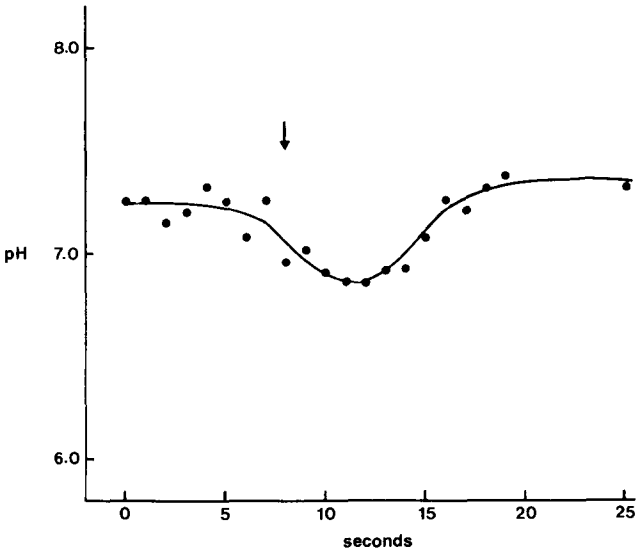

FIGURE 4 Cytoplasmic pH vs. time during the wound-healing response in a typical experiment. The spot observed is a 50 μm diameter area on the side of an advancing pseudopod of an FTC-ovalbumin-injected ameba. Upon damage by puncture (arrow), the pH drops from 7.25 to 6.90 within 5 s, then recovers to its original value within another 5 s.

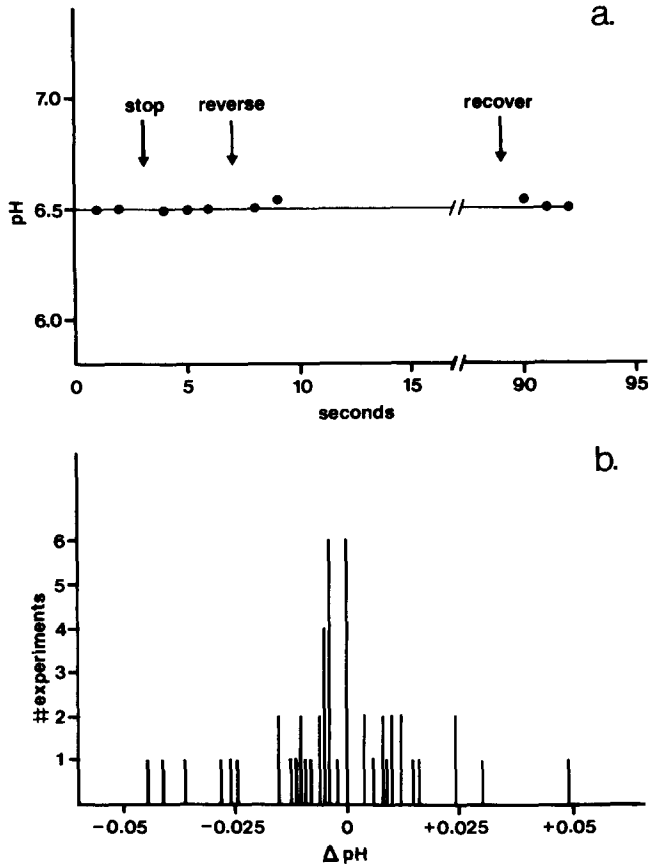

FIGURE 5 Comparison of cytoplasmic pH in tails and advancing pseudopod tips in freely moving FTC-ovalbumin-injected specimens of *C. carolinensis*. (*a*) A typical time-course (pH vs. s) of pH during the light-induced reversal and subsequent recovery of an advancing pseudopod. Spot size, 50 μm (see Fig. 1). Arrows mark the various relevant events: when streaming stops, when it reverses, and when the pseudopod recovers its original direction of streaming. The pH remains constant throughout the experiment. See text for further details. (*b*) A bar graph summarizing the distribution of observed differences in pH ($pH_{pseudopod} - pH_{tail}$) among 49 pairs of tails and pseudopod tips (No. experiments) in 12 amebae. The average ΔpH is −0.02 U, which is not significant.

In the second type of experiment, pairs of tail and tip measurements were made in moving monopodial amebae by measuring the tail for 3 s, then quickly moving to the tip and measuring again for 3 s (at which point the tip usually stopped). Figure 5 *b* shows a bar graph of the distribution of pH differences ($pH_{pseudopod}$-pH_{tail}) observed. A weighted average of all such pair measurements (49 trials, 12 cells) yields a mean and median ΔpH of only −0.02 U. This difference does not exceed the average variation (±0.02 U) observed for tails or pseudopods themselves during these experiments.

DISCUSSION

Average Cytoplasmic pH in Chaos

The average cytoplasmic pH of 6.75 that we have determined for *Chaos* is lower than most previously reported values (2, 11). There are two possible reasons for this discrepancy. First, the classical values come from subjective evaluation of the color of an injected pH-indicator dye, which partitions rapidly into all cellular compartments. Because *Chaos* contains hundreds of nuclei and other organelles, which seem to have a higher pH than the cytoplasm (2), it is no surprise that the average pH observed using this technique (6.9–7.6) is higher than the value we obtain for cytoplasm alone. Interestingly, by observing only the clear hyaline zone of amebae injected with dye before (2) or after (34) centrifugation to stratify organelles, similar cytoplasmic pH values of 6.6–6.8 have been obtained for *Amoeba dubia*. The second reason for the discrepancy may simply be that previous calibration of dyes was done by comparison with standards in solution. As demonstrated here and by other investigators (18, 29), this may result in serious errors. In this case, we would report much higher average cytoplasmic pHs if we calibrated the signals with the standard curve in solution (cf. Fig. 3 *a* and *b*). The precise reason for the altered behavior of the probe *in situ* is unknown, but fluorescence is known to be sensitive to environmental factors (14).

Significantly, the average cytoplasmic pH value we observe (6.75) corresponds to the pH optimum of 6.8 found for Ca^{++} regulation of a partially-purified motile model from *Dictyostelium discoideum* amebae (10). At this pH, solation, gelation, and contraction of the extract is regulated by changes in free Ca^{++} concentration in the submicromolar range. This pH is also near the value (7.0), which allows similar regulation of viscoelasticity and contractility in isolated cytoplasm of *Chaos* (27). Furthermore, a distinct difference in cytoplasmic structure and contractility between amebae subjected to pHs at or below 6.8 (which favors a gelled state) and those subjected to pHs above 6.8 (which favors contraction) is observed during generation of the *in situ* standard curve. Thus, the significance of this pH value for regulation of structure and contractility of ameba cytoplasm is strongly suggested.

We note a great deal of variation both within a single cell (differences of up to 0.4 U) and between cells (a range of 6.3–7.4, see Fig. 3, *inset*). Furthermore, average pH values appear to cluster into two groups (Fig. 3, *inset*), one around pH 6.5, the other around pH 6.8. These variations could have some biological significance, and we have initiated studies to correlate them with cellular events. pH may be important in the regulation of metabolism and general level of motile activity throughout the life cycle of the ameba. Oscillations in intracellular pH during the life cycle of the acellular slime mold, *Physarum polycephalum*, have been reported (7), and intracellular pH changes have been shown to activate protein synthesis in developing sea urchin eggs (9). It is well known that the motile activity of the free-living amebae varies with physiological state (11), especially with respect to feeding and division, both of which induce fairly quiescent states. Average cytoplasmic pH may vary with different phases of the life cycle of the ameba and could have some effect on motile activity. Synchronized cell cultures should shed some light on this possibility.

The Wound-healing Response

Wound-healing in the giant amebae is a well-documented contractile event (28). After damage by puncture, amebae preinjected with 5-iodoacetamidofluorescein-labeled actin show a local transient increase in actin concentration at the wound site (28). Similarly, amebae preinjected with aequorin, when punctured, luminesce at the site of injury, indicating a local increase in free Ca^{++} (25). Previous studies with absorbant dyes suggested the presence of an "acid of injury" in amebae, similar to that known to exist in other cells (2), and we have detected local, transient pH decreases of as much as 0.35 U during wounding. The magnitude of the local pH drop may be greater than that observed because some uninjured cytoplasm is usually included in the measuring spot. Values obtained will always be an average of the pH of all regions within the spot.

Nevertheless, *Chaos* recovers extremely rapidly (within 5–10 s) to the predamaged pH value (see Fig. 4), suggesting powerful pH-homeostasis mechanisms within the cell.

Comparison of Tails and Pseudopods

We have investigated the possibility that proton fluxes, perhaps measurable as pH changes, play an important regulatory role in ameboid movement. We have compared matched pairs of tails and pseudopods in 12 different freely moving, monopodial amebae and we have measured pseudopods during cycles of light-induced arrest, reversal, and recovery. In no case is any consistent evidence found for the correlation of pH changes with morphology or movement at our current level of spatial (50 μm) and temporal (1.3 s) resolution. However, we cannot rule out regulatory changes confined to smaller domains (e.g., a narrow margin of the cell cortex) or of much shorter duration, either of which could be obscured by our present methods.

Several lines of evidence suggest that ameboid movement may be dually regulated by Ca^{++} and pH. External Ca^{++} is absolutely required for sustained locomotion (11). Moreover, occasional spikes of current entering pseudopod tips, as measured with an extracellular vibrating probe (16), and spontaneous bursts of luminescence observed in pseudopod tips of amebae injected with aequorin (25), both require external Ca^{++}. Ca^{++} has also been shown to carry part of a steady current that enters the tails of *Chaos* (16), though the persistence of this current at a reduced level, in the absence of external Ca^{++}, suggests that it is carried in part by other ions. While ion substitution experiments rule out the involvement of other divalent cations, a role for protons is suggested by experiments in which the current reduction upon removal of external Ca^{++} is prevented by simultaneously lowering the pH of the medium (16). In addition, external pH has been shown to affect ameba morphology and rate of movement (11).

Quantitation of aequorin luminescence in ameba tails reveals that movement occurs at free Ca^{++} concentrations between 1.0×10^{-7} and 1.0×10^{-6} M (25). This range was first shown to regulate the gelation-solation-contraction cycle in ameba cytoplasm (27) and has since been shown to regulate structure in other cytoplasmic contractile protein preparations (15, 19, 35). However, it has also been shown (4, 10) that increasing the pH of a motile extract above the optimal value for gelation (at subthreshold levels of free Ca^{++}) will increasingly favor solation and contraction of the gel until a pH value is reached (usually around 7.5) at which gelation is inhibited completely, and only contraction occurs. (Aequorin studies show that free Ca^{++} remains at subthreshold concentrations during these experiments [4].) The existence of this "graded response" of cytoplasmic extracts has intriguing implications for cellular regulation of motility. Because we do observe variations in cytoplasmic pH within cells, and between cells, that range above and below this optimal value, pH may be a cellular mechanism for "fine-tuning" contractility. Support for this hypothesis also comes from the behavior of amebae when equilibrated or injected with buffers of varying pHs during generation of the *in situ* standard curve (see above).

Work is in progress to improve the resolution of our present technique by decreasing the measuring spot size, increasing the sensitivity of photodetection, and by application of image analysis techniques to image intensified video recordings. We are also extending the technique to studies in other cells and cell processes, including capping and endocytosis in amebae and cortical activation and division in sea urchin eggs.

Special thanks to Bob Zeh for his invaluable expertise and time spent designing and constructing equipment with us. We would also like to thank R. Calabrese, V. Fowler, S. B. Hellewell, E. Luna, and Y.-L. Wang for helpful discussions of, and critical comments on, the work and manuscript. We thank Lisa Houck for the figures.

This work was supported by a National Institutes of Health (N. I. H.), Institute of Arthritis, Metabolism, and Digestive Diseases Research Grant (AM 18111), a National Science Foundation Grant (PCM 7822499) to Dr. Taylor, and by a National Institutes of Health Predoctoral Training Grant (GM 07598) to Ms. Heiple.

Received for publication 20 March 1980, and in revised form 2 June 1980.

REFERENCES

1. Begg, D. A., and L. I. Rebhun. 1979. pH regulates the polymerization of actin in the sea urchin egg cortex. *J. Cell Biol.* 83:241–248.
2. Chambers, R., and E. L. Chambers. 1961. Explorations Into the Nature of the Living Cell. Harvard University Press, Cambridge.
3. Condeelis, J. S. 1977. The isolation of microquantities of myosin from *Amoeba proteus* and *Chaos carolinensis*. *Anal. Biochem.* 78:374–394.
4. Condeelis, J. S., and D. L. Taylor. 1977. The contractile basis of amoeboid movement V. The control of gelation, solation, and contraction in extracts from *Dictyostelium discoideum*. *J. Cell Biol.* 74:901–927.
5. Deamer, D. W., R. C. Prince, and A. R. Crofts. 1972. The response of fluorescent amines to pH gradients across liposome membranes. *Biochim. Biophys. Acta.* 274:323–335.
6. Eisenbach, M., H. Garty, E. P. Bakker, G. Klemperer, H. Rottenberg, and S. R. Caplan. 1978. Kinetic analysis of light-induced pH changes in bacteriorhodopsin-containing particles from *Halobacterium halobium*. *Biochemistry.* 17:4691–4697.
7. Gerson, D. F., and A. C. Burton. 1976. The relation of cycling of intracellular pH to mitosis in the acellular slime mould *Physarum polycephalum*. *J. Cell Physiol.* 91:297–304.
8. Gilkey, J. C., L. F. Jaffe, E. B. Ridgway, and G. T. Reynolds. 1978. A free calcium wave traverses the activating egg of the medaka, *Oryzias latipes*. *J. Cell Biol.* 76:448–466.
9. Grainger, J. L., M. M. Winkler, S. S. Shen, and R. A. Steinhardt. 1979. Intracellular pH controls protein synthesis rate in the sea urchin egg and early embryo. *Dev. Biol.* 68:396–406.
10. Hellewell, S. B., and D.L. Taylor. 1979. The contractile basis of ameboid movement VI. The solation-contraction coupling hypothesis. *J. Cell Biol.* 83:633–648.
11. Jeon, K. W. 1973. The Biology of Amoeba. K. W. Jeon, editor. Academic Press, Inc. N. Y.
12. Johnson, J. D., D. Epel, and M. Paul. 1976. Intracellular pH and activation of sea urchin eggs after fertilization. *Nature (Lond.).* 262:661–664.
13. Kano, I., and J. H. Fendler. 1978. Pyranine as a sensitive pH probe for liposome interiors and surfaces. pH gradients across phospholipid vesicles. *Biochim. Biophys. Acta.* 509:289–299.
14. Martin, M. M., and L. Lindqvist. 1975. The pH dependence of fluorescein fluorescence. *J. Lumin.* 10:381–390.
15. Mimura, N., and A. Asano. 1979. Ca^{2+}-sensitive gelation of actin filaments by a new protein factor. *Nature (Lond.).* 282:44–48.
16. Nuccitelli, R., M. Poo, and L. F. Jaffe. 1977. Relations between amoeboid movement and membrane-controlled electrical currents. *J. Gen. Physiol.* 69:743–763.
17. Ohkuma, S., and B. Poole. 1978. Fluorescence probe measurement of the intralysosomal pH in living cells and the perturbation of pH by various agents. *Proc. Natl. Acad. Sci. U. S. A.* 75:3327–3331.
18. Pollard, H. B., H. Shindo, C. E. Creutz, C. J. Pazoles, and J. S. Cohen. 1979. Internal pH and state of ATP in adenergic chromaffin granules determined by ^{31}P nuclear magnetic resonance spectroscopy. *J. Biol. Chem.* 254:1170–1177.
19. Pollard, T. D. 1976. The role of actin in the temperature-dependent gelation and contraction of extracts of *Acanthamoeba*. *J. Cell Biol.* 68:579–601.
20. Rubin, R. P. 1974. Calcium and the Secretory Process. Plenum Press, New York.
21. Shen, S. S., and R. A. Steinhardt. 1978. Direct measurement of intracellular pH during metabolic derepression of the sea urchin egg. *Nature (Lond.).* 272:253–254.
22. Stacey, D. W., and V. G. Allfrey. 1977. Evidence for the autophagy of microinjected proteins in HeLa cells. *J. Cell Biol.* 75:807–817.
23. Steinhardt, R., R. Zucker, and G. Schatten. 1977. Intracellular calcium release at fertilization in the sea urchin egg. *Dev. Biol.* 58:185–196.
24. Taylor, D. L. 1976. Quantitative studies on the polarization optical properties of striated muscle. *J. Cell Biol.* 68:497–511.
25. Taylor, D. L., J. R. Blinks, and G. Reynolds. 1980. The contractile basis of ameboid movement. VIII. Aequorin luminescence during ameboid movement, endocytosis, and capping. *J. Cell Biol.* 86:599–607.
26. Taylor, D. L., and J. S. Condeelis. 1978. Cytoplasmic structure and contractility in amoeboid cells. *Int. Rev. Cytol.* 56:57–144.
27. Taylor, D. L., J. S. Condeelis, P. L. Moore, and R. D. Allen. 1973. The contractile basis of amoeboid movement. I. Chemical control of motility in isolated cytoplasm. *J. Cell Biol.* 59:378–394.
28. Taylor, D. L., Y.-L. Wang, and J. M. Heiple. 1980. The contractile basis of ameboid movement. VII. Distribution of fluorescently labeled actin in living amebae. *J. Cell Biol.* 86:590–598.
29. Thomas, J. A., R. N. Buschbaum, A. Zimniak, and E. Racker. 1979. Intracellular pH measurements in Ehrlich ascites tumor cells utilizing spectroscopic probes generated *in situ*. *Biochemistry.* 18:2210–2218.
30. Tilney, L. G., D. P. Kiehart, C. Sardet, and M. Tilney. 1978. Polymerization of actin. IV. Role of Ca^{++} and H^+ in the assembly of actin and in membrane fusion in the acrosomal reaction of echinoderm sperm. *J. Cell Biol.* 77:536–550.
31. Waddell, W. J., and R. G. Bates. 1969. Intracellular pH. *Physiol. Rev.* 49:285–329.
32. Wang, Y.-L., and D. L. Taylor. 1979. Distribution of fluorescently labeled actin in living sea urchin eggs during early development. *J. Cell Biol.* 81:672–679.
33. Weber, A., and J. M. Murray. 1973. Molecular control mechanisms in muscle contraction. *Physiol. Rev.* 53:612–673.
34. Wiercinski, F. J. 1944. An experimental study of protoplasmic pH determination. I. *Amoebae* and *Arbacia punctulata*. *Biol. Bull.* 86:98–112.
35. Yin, H. L., and T. P. Stossel. 1979. Control of cytoplasmic actin gel-sol transformation by gelsolin, a calcium-dependent regulatory protein. *Nature (Lond.).* 281:583–586.